Adaptive introgression during environmental change can weaken reproductive isolation

Gregory L. Owens[1]*, *Kieran Samuk*[2]

[1] Department of Integrative Biology, University of California, Berkeley. Berkeley, California, USA, 94720; Department of Botany, University of British Columbia, Vancouver, BC, Canada.

[2] Department of Biology, Duke University. Durham, NC, USA, 27708.

*Corresponding author, gregory.lawrence.owens@gmail.com

Abstract

Anthropogenic climate change is an urgent threat to species diversity. One aspect of this threat is the collapse of species reproductive barriers through increased hybridization. The primary mechanism for this collapse is thought to be the weakening of ecologically-mediated reproductive barriers, as demonstrated in many cases of "reverse speciation". Here, we expand on this idea and show that adaptive introgression between species adapting to a shared, moving climatic optimum can readily weaken *any* reproductive barrier, including those that are completely independent of the climatic variable. Using genetically explicit forward-time simulations, we show that genetic linkage between alleles conferring adaptation to a changing climate and alleles conferring reproductive isolation can lead to adaptive introgression facilitating the homogenization of reproductive isolation alleles. This effect causes the decay of species boundaries across a broad and biologically-realistic parameter space. We explore how the magnitude of this effect depends upon the rate of climate change, the genetic architecture of adaptation, the initial degree of reproductive isolation and the mutation rate. These results highlight a previously unexplored effect of rapid climate change on species diversity.

Introduction

Global climate change (GCC) is expected to be an increasingly important stressor in the next century (Thomas et al. 2004, Hoffmann and Sgro 2011). GCC can lead to significant fitness costs or extinction if populations cannot shift their ranges or adapt to

the changing climate (Jump and Penuelas 2005; Zimova et al. 2016). Apart from its direct effects, GCC can also profoundly alter ecological context via changes in phenology or species composition (Walther et al. 2002). As such, GCC represents an existential threat to biological diversity, at the level of populations, species, and ecosystems. Considering the central role of biological diversity in the functioning of evolutionary and ecological processes, understanding the full biological effect of GCC is a key problem.

One potential effect GCC is an increase in inter-species hybridization, which can itself precipitate further loss of biodiversity (Rhymer and Simberloff 1996, Todesco et al. 2016). Such hybridization can cause a common species to subsume a rare species (Oliveira et al. 2008; Beatty et al. 2014; Vallender et al. 2007) or the collapse of multiple species into a single hybrid swarm (Taylor et al. 2006). In both cases, unique adaptive combinations of alleles and discrete species are lost. GCC may increase this threat by breaking down spatial, temporal or behavioural premating barriers (Chunco 2014). At the simplest level, range shifts can bring together species that may have no other significant barriers (e.g. Garroway et al. 2010). Reproductive barriers relying on the timing of life-history events are also susceptible to climate change which can increase the temporal overlap between species (e.g. Gerard et al. 2006). Furthermore, behavioural isolation may rely on environmental cues disrupted by GCC, such as in spadefoot toads in which water conditions influence mate choice (Pfennig 2007). The breakdown of these barriers may lead to loss of more rare species under GCC, or the collapse of sister species, as has been seen in smaller localized environmental shifts (Taylor et al. 2006; Vonlanthen et al. 2012).

Hybridization can also facilitate adaptation to GCC through the transfer of adaptive alleles between species, i.e. adaptive introgression. This has traditionally been studied in the context of species/populations with pre-existing differential adaptation to the changing climate variable; for example a warm adapted species transfering alleles to a cold adapted species (e.g. Gómez et al. 2015). In this example, one species acts as a pool of alleles preadapted to the future climate. Importantly, in this case introgression (with its potential negative side effects) is being driven by selection and not demographic processes or perturbations of prezygotic isolation.

Hybrid zone models have also shown that universally adaptive alleles readily introgress across hybrid zones, while alleles that cause reproductive isolation generally resist introgression (Barton 1979, Gompert et al. 2012, Barton 2013). Further, depending on the balance between reproductive isolation and shared ecological selection, introgression can cause previously isolated populations to remain isolated or collapse into hybrid swarms (e.g. Burkele 2000).

What has not been appreciated in previous models is that during a rapid environmental shift, segregating variation within two reproductively isolated species may undergo adaptive introgression in spite of linkage to reproductive isolation alleles. This process could occur if the fitness benefit of a particular allele outweighs the fitness cost of any linked alleles. As such, adaptive introgression could drive speciation reversal even when neither species is strongly preadapted to the environmental shift and when reproductive isolation is initially strong.

Here we extend the idea of adaptive introgression to species whose reproductive barriers are uncorrelated with environmental variables related to GCC. In this case, two

species that are initially reproductively isolated but remain capable of hybridization must cope with an extreme shift in the environment. We explore the parameter space for cases where adaptation to a shifting climatic optimum drives a reduction in reproductive isolation. We probe this idea using forward-time population genetic simulations and answer two questions: (I) Does rapid environmental change allow introgression to occur in the face of reproductive isolation? (II) If so, what is the parameter space where it occurs? We interpret these results in the context of the future anthropogenic climate change and the loss of species diversity.

Methods

Conceptual model

We consider the scenario of two parapatric species inhabiting demes host to different abiotic variables. These species exchange migrants at a low level, but reproductive isolation via local adaptation (i.e. extrinsic postzygotic isolation and immigrant inviability) is strong enough to prevent substantial introgression. We imagine that these two species must also cope with constant adaptation to a shared oscillating "climate" optimum. This oscillation continues for a long initial burn in period, during which alleles conferring adaptation to climate accumulate in each species. After this period, oscillation ends and the climatic optimum rapidly increases at a constant rate, as is expected under projections of anthropogenic climate change.

We hypothesize that if the rate of change in the climatic optimum is sufficiently high, selection for migrant alleles conferring increased climate tolerance will overwhelm the negative fitness effects of linked reproductive isolation alleles. This will

cause the erosion of reproductive isolation between species and increase the chance of speciation reversal. Importantly, we expect this outcome even when the strength of ecological selection mediating reproductive isolation itself is orthogonal to the strength of climate-mediated selection.

Model details

We implemented the above conceptual model as a genetic explicit Wright-Fisher model in SLiM 3.0 (Haller and Messer 2018). The details of this model are depicted graphically in Figure 1 and the simulation parameters and their values are detailed in Table 1. We simulated two populations of constant size *Ne,* with a constant migration rate of *m* proportion migrants per generation. Each individual was initialized with 99999 loci contained on a single chromosome with a uniform recombination rate of *r* between loci. We initially scaled the recombination rate so that the entire genome was 100 cM in length, but varied recombination rate up a genome size of 1000 cM. Since each population represented a locally adapted species, we added n_{RI} divergently selected alleles at loci evenly spaced across the chromosome, with each population fixed for a different allele. Divergently selected alleles imposed a fitness cost of $s_{RI} = s_{Total}/n_{RI}$ when not found in its original population, modelling extrinsic postzygotic isolation. Ancestry was tracked by using 100 neutral alleles initially fixed between the populations, spread evenly across the genome.

Fitness also depended on phenotypic distance from the climatic optimum. This optimum was initially 0, and during the burn in period oscillated from -5 to 5 every 500 generations based on the formula: $5 * cos(generation - 250)/(\pi * 50)$. Individual

phenotype was determined by alleles at QTL-like climate loci which could appear via mutation at all sites not inhabited by a divergently selected or ancestry tracking site (i.e. 99899 - n_{RI} sites). These mutations occurred at a rate μ per base position per sample per generation and their phenotypic effect was drawn from a gaussian distribution with a mean of zero and a standard deviation of QTL_{SD}. The QTL climate alleles modify whether an individual is hot or cold adapted but does not broaden their climate niche.

We ran a burn in of $10Ne$ generations to build up sufficient standing variation and then the complete state of each replicate simulation was saved. Each simulation was then continued under both a control and climate change scenario for an additional 100 generations. In the control scenario, environmental oscillation continued as normal while in the climate change scenario the phenotypic optimum increased by a rate of Δ each generation without oscillation. For every generation we recorded the average reproductive isolation, the mean fitness, the mean and standard deviation of the climate phenotype and the amount of introgressed ancestry for each population. Finally, for each simulation we report the change in mean introgressed ancestry and reproductive isolation between the start and end of control and test scenarios, as well as the mean evolutionary rate, in Haldanes, for the test scenario. Reproductive isolation was measured by calculating the average fitness penalty from RI alleles based on RI allele frequencies. All formulas used in the simulation are presented in Supplementary Appendix 1 and all code used is available at https://github.com/owensgl/adaptive_introgression.

To explore the parameter space under which adaptive introgression mediated RI collapse, we systematically varied the following parameters: mutation rate (μ), migration

rate (m), strength of divergent selection (s_{Total}), the number of divergently selected loci (n_{RI}), the standard deviation of QTL effect sizes (QTL_{SD}) the recombination rate (r), and the rate of climate change (Δ). We varied each parameter independently and kept the other parameters at a default value known to permit a low level of introgression in preliminary tests (Table 1). A plotting was done using ggplot2 (Wickham 2016).

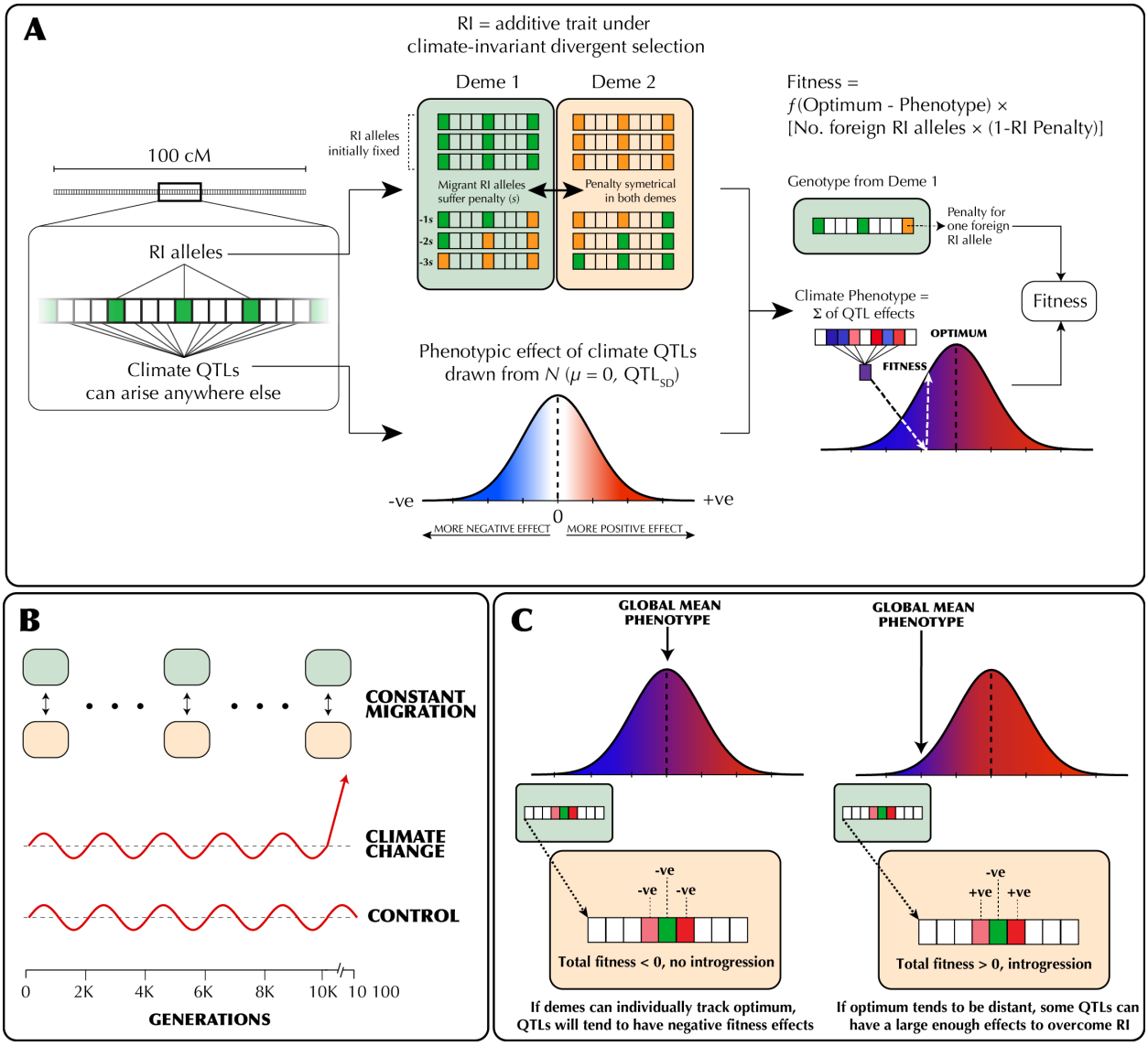

Figure 1 | (A) The genetic architecture of adaptation and speciation in the model. From left to right: Each individual has a single 100-1000 cM chromosome, over which reproductive isolation (RI) loci occur at

regularly-spaced intervals. These loci are initialized with RI alleles (at 100% frequency) that confer local adaptation to one of two initial demes (depicted as green or orange alleles, corresponding to deme 1 or deme 2 environments). Both demes are of equal size (Ne = 1000). All non-RI loci (depicted as white/transparent loci, initially) have the potential to give rise to climate-adaptation alleles. The phenotypic effects of each these alleles are drawn from a normal distribution (shown as a gradient from blue to white to red). An individual's climate phenotype is the sum of the phenotypic effects of its climate QTLs (pure additivity). The fitness of each individual is a function of the number of foreign RI alleles and the phenotypic distance of that individual from the environmental optimum, with the climate fitness landscape modelled as a gaussian distribution (shown as a gradient from blue to red). (B) The course of the simulation. Migration rate and population size of the two demes is held constant. In each replicate simulation, the fitness optimum fluctuates regularly a 10 000-generation burn-in period. The state of the initial populations is then duplicated and subjected to 100 additional generations of (1) a climate change scenario in which the climatic optimum rapidly shifts in a single direction and (2) a control scenario in which the optimum continues its fluctuation course. (C) The conditions under which adaptive introgression overwhelms RI. On the left, if the two populations are able to individually track the climatic optimum, newly-arising climate alleles are only able to exert either weakly positive or (more commonly) negative effects on fitness due to overshooting the optimum. In contrast, on the right, if the populations cannot effectively track the optimum (e.g. due to mutational limitations and/or a rapidly shifting optimum), there is scope for climatic alleles to have large positive fitness effects. If these fitness effects are sufficient large, these alleles can overwhelm the negative fitness effects of linked RI alleles and introgress between demes, degrading overall reproductive isolation.

Table 1 | Parameters of the adaptive introgression simulations. For each set of simulations, each parameter was set to the starting value which was varied from the minimum to maximum value by the specified increment.

Parameter	Symbol	Starting value	Range, Increment
Migration rate (proportion migrants/generation)	m	0.01	0.0-0.1, 0.001
Total strength of RI	s_{Total}	0.9	0.1-1, 0.01
Number of RI loci	l_{RI}	100	5-100, 5
Mutation rate (mutations/sample/locus/generation)	μ	1e-7	$1e^{-8}$-$5e^{-7}$, $1e^{-8}$
Climate QTL standard deviation	QTL_{SD}	1	0.1-5.0, 0.1
Rate of climate change	Δ	1	0.1-3, 0.1
Recombination rate	r	1e-5	$1e^{-5}$-$5e^{-5}$, $1e^{-6}$

Parameter	Symbol	Starting value	Range, Increment
Population size	N_e	1000	-
Environmental fitness standard deviation	$sd_{climate}$	2	-
Burn in generations	-	10000	-
Shift generations	-	100	-
Replicates	-	100	-
Loci on chromosome	-	99999	-
Burn in oscillation rate	f	1000	-
Burn in oscillation height	a	5	-

Results

Rapid climate change and adaptive introgression facilitates collapse of species boundaries

When climate change is rapid, we find that adaptive introgression of climate alleles rapidly drives the homogenization of allele frequencies at RI loci between species. Figure 2 visualizes one example simulation where after 100 generations of climate change, RI is degraded to half its original strength (Figure 2A) and a substantial proportion of climate alleles are of migrant origin (Figure 2D). As QTL climate loci alleles between populations, RI and neutral alleles hitchhike with them leaving substantial introgression (Figures 2B-C). In contrast, RI remains intact and introgression is minimal in the paired control scenario without climate change (Figure S1).

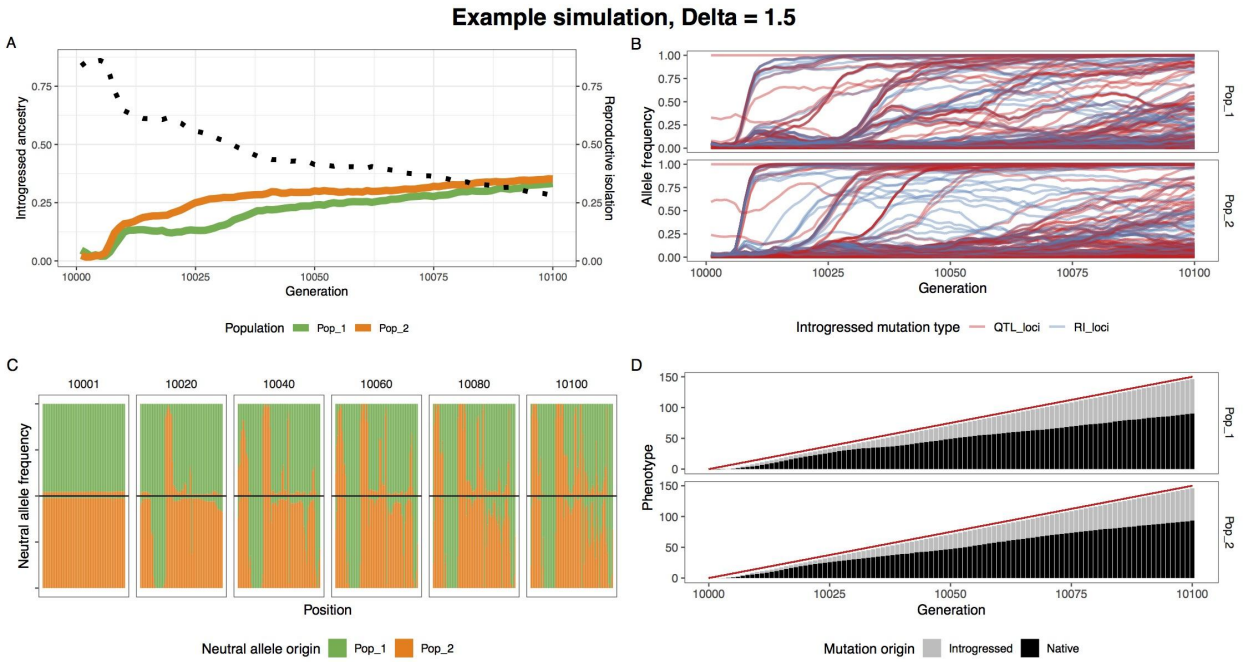

178 **Figure 2** | A single example simulation with $\Delta = 1.5$, illustrating the climate driven adaptive introgression.
179 (A) The average introgressed ancestry for each population (orange and green) and the average
180 reproductive isolation between populations (black dotted). (B) The allele frequency trajectory for
181 introgressed climate QTL (red) and RI (blue) alleles. It highlights how RI alleles rise to high frequency in
182 conjunction with climate QTL alleles. (C) Ancestry for neutral loci during the post-burn in period at 20
183 generation intervals. The top and bottom halves of the figure represent population 1 and 2 respectively.
184 (D) The optimum phenotype (red line) and the summed phenotypic effect for introgressed and native loci.
185

186 For a wide range of parameters we find decreased reproductive isolation and
187 increased introgressed ancestry in the test climate change scenario (Figures 3 and S2).
188 This effect is enhanced by reduced levels of genetic variation; both reducing mutation
189 rate and reducing the standard deviation of the climate QTL effect size increases the
190 likelihood and magnitude of adaptive introgression. As expected, increasing migration
191 rate increases the RI decay. Increasing the strength of divergent selection between
192 species decreases the amount of adaptive introgression, although a signal is still visible
193 even when the strength of total divergent selection is 0.99. Below 0.5 total divergent
194 selection and above 0.07 migration rate, both species collapse into a hybrid swarm

during the burn in period, so adaptive introgression is not relevant. Increasing number of RI loci while keeping the strength of total RI, and decreasing the recombination rate both increased the amount of RI lost. Lastly, increasing the rate of climate change in the test scenario increases the amount of adaptive introgression.

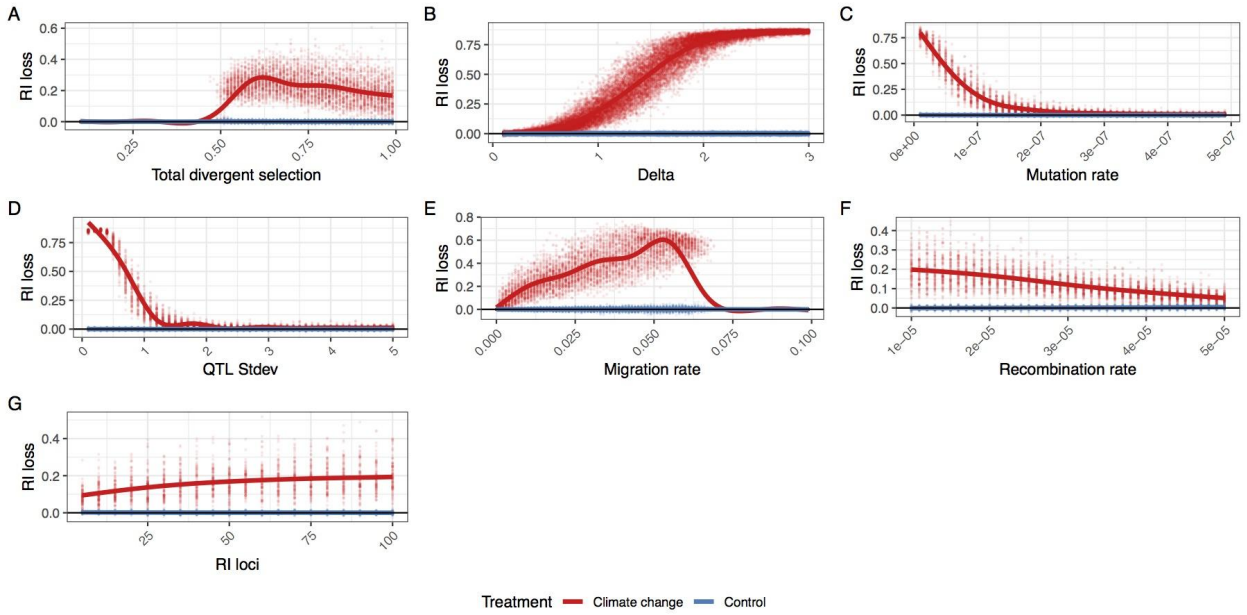

Figure 3 | The average loss of reproductive isolation at the end of the post-burn in period. Each replicate simulation is represented by two points, one with simulating climate change (red) and one with an extension of the burn in oscillation (blue). Individual parameters were varied to show the effect of (A) total divergent selection, (B) optimum shift per generation (delta), (C) climate QTL mutation rate, (D) climate QTL effect size standard deviation, (E) migration rate, (F) the recombination rate and (G)) the number of reproductive isolation loci. The maximum loss of reproductive isolation is 0.9 ($1\text{-}s_{Total}$) for most simulations, except when total divergent selection is varied.

Simulation parameters fall within realistic ranges

To better connect our simulation results with observations from natural populations, we measured the rate of phenotypic evolution in the test scenario in Haldanes (standard deviations per generation). We find that most simulations had average evolutionary rates ranging from 0.01 to 0.06 Haldanes and are within the range

of empirical estimates (Hendry et al. 2008), with the exception of simulations varying Δ (Figure S3). For very large values of Δ (>2.5), we found large and erratic evolutionary rates. For many of these simulations, one or both species failed to track the changing environment causing fitness to fall to zero and end the simulation.

Discussion

Climate change is expected to have detrimental effects on diversity, but the incidental effects of adaptive introgression have not been previously explored. Our simulations have shown that it is possible for adaptation to a common changing environment to cause introgression and speciation reversal, even when the form of RI is not directly affected by the changing environment.

Will adaptive introgression lead to speciation reversal?

Several parameters had a strong effect on the amount of introgression. When adaptive variation is limited, reproductive isolation is minimal or environment change is fast, complete genetic homogenization is likely. In these cases, reproductive isolation is completely removed and would clearly represent speciation reversal if seen in nature. For much of the parameter space, introgression is increased during environmental change, but populations do not completely homogenize. In these cases, reproductive isolation is still reduced between populations (Figure 3) and it is important to note that our simulations do not consider additional factors that would be lead to species collapse. We simulate RI loci that are extrinsic and not epistatic, thus provide constant selection against introgressed ancestry. If RI is largely epistatic, selection against

introgressed ancestry can decline or reverse as introgression increases (note that this would result in the collapse of RI being even more intense). Furthermore, we simulated population sizes as equal and constant. Unbalanced population sizes may result in one population harboring more adaptive alleles and lead to unbalanced introgression. Small populations are also more susceptible to extinction due to the fitness costs of introgressed RI alleles.

The ultimate question of which species are in danger of reverse speciation is dependent on a multitude of interacting factors and is beyond the scope of this paper, but we can highlight several risk factors.

(1) For hybridization to be an issue, a potential hybridizing species must be at least in parapatry. Surveys have estimated the percent of species that hybridize with at least one other congener to be around 10-25%, although if climate change disrupts species ranges or premating isolation, that number may increase (Mallet 2005).

(2) The speed of environment changes and the steepness of the changing fitness landscape. Species with wide climate niches will be less susceptible because they will be under weaker selection.

(3) The genetic architecture of climate adaptation in the species. Species with large numbers of large effect climate adaptation alleles segregating within the gene pool will be more able to adapt to the changing climate without introgressed alleles. Low diversity species will be more susceptible and reliant on adaptive introgression.

(4) The genetic architecture of reproductive isolation between species. Species with few large effect RI loci will be more resistant to RI decay than species with a more diffuse polygenic RI architecture.

Implications for the fate of species in changing environments

Our simulations suggest that rapidly changing environments can cause the collapse of species barriers in the *absence* of any direct effect on the underlying strength of reproductive isolation. By design, we modelled a scenario in which the strength of RI (modelled as divergent selection) is (a) invariant throughout (i.e. not reduced by environmental change itself) and (b) totally orthogonal to the strength of climate-mediated selection. This is an important departure from previous work, in which the collapse of reproductive isolation or "reverse speciation" occurs because RI is itself dependent on the environment (e.g. trophic or sensory niche).

This difference has several important implications. For one, the mechanism we outline here can occur in any population where adaptive introgression is possible (i.e. RI is not absolute and the climate mediated selective optimum is to some degree shared). This greatly expands both the number of populations that may be susceptible to introgressive collapse and the potential severity of such collapses. For example, adaptive introgression could act in concert with the collapse of climate-mediated reproductive barriers, accelerating collapse. Further, while not directly studied here, this mechanism could in theory mediate the collapse of RI even when all reproductive barriers are independent of ecological context (e.g. in the case of purely intrinsic isolation).

Although we have framed our discussion in the context of climate change, this is applicable to any strong consistent shared selective event. These events include any environmental or ecological disturbance that alters the shared selective landscape of the two populations such that both populations are sufficiently displaced from their selective optima (thereby increasing the average size of selection differentials between genotypes, i.e. the strength of selection). One such event that has been studied in natural systems is eutrophication, which has been suggested to have caused speciation reversal in European lake whitefish (Vonlanthen et al. 2012). Thus far, this reversal has been attributed to changes in RI as a direct result of ecological and/or behavioural changes. However, if eutrophication exerts a common selective pressure on a group of parapatric species (e.g. mediated through changes in water chemistry) introgression could become adaptive and contribute to the collapse of species boundaries. Similarly, ocean acidification could be a strong source of shared selection and may induce introgression between previously well isolated species (Pespeni et al. 2013).

In contrast to our hypothesis of introgression driving species collapse, adaptive introgression of an insecticide-resistance mutation in *Anopheles* mosquitoes lead to the homogenization of previously differentiated genomic region, but not genome wide despeciation (Clarkson et al. 2014). In this example, selection seemingly only acts on a single large effect locus, rather than the polygenic architecture of climate adaptation we hypothesize. This limits the amount of introgression in comparison to our simulations and highlights the importance of the genetic architecture of climate adaptation.

Linkage and the genetic architecture of climate adaptation

A key aspect of our model is that while RI loci occur at predefined intervals in the genome, climate-sensitive alleles can arise at any other locus in the genome. This allows for climate-sensitive alleles to become readily linked to RI-causing alleles and eventually introgress if the combined effect of positively selected climate alleles exceeds the deleterious effect of the linked RI allele. The incidental establishment of this linkage within the two adapting populations is a fundamental cause of later introgressive collapse. This is supported by our simulations where varied the number of RI loci and also incidentally varied the average degree of linkage between all climate-sensitive loci and all RI loci. We found that in simulations with more RI loci, and therefore a higher probability of linkage between RI and climate-sensitive loci, there was greater loss of reproductive isolation. Thus, a key question is whether such linkage could plausibly be established in a natural population.

Several lines of evidence suggest that this is likely to be true. First, the genetic architecture of adaptation to a changing climate is likely to closely resemble the architecture of local adaptation in general, i.e. a large number of small effect alleles with a smaller number of large effect loci (reviewed in Savolainen et al. 2013). This idea is directly supported by recent working showing that climatic adaptation in conifers is underlain by large number of loci scattered throughout the genome, with the majority of these showing modest phenotype-environment correlations (Yeaman et al. 2016). Secondly, recent analyses of large human datasets support the idea that most complex traits (of any kind) are probably determined by a large number of small-effect loci found nearly everywhere in genome along with a handful of “core genes” (Boyle et al. 2018). Thus, given that the genetic architecture of RI is itself likely to be highly polygenic

(discussed in Ravinet et al. 2017), it seems highly plausible that linkage between climate-sensitive alleles and RI alleles can readily occur in natural populations.

The role of recombination rate

Recombination rate is thought to play a key role in mediating patterns of divergence and introgression in natural populations (e.g. Samuk et al. 2017, Schumer et al. 2018). Specifically, regions of low recombination are thought to be more resistant to gene flow because of increased linkage between alleles conferring RI. Here, we modelled a chromosome with a uniform recombination profile, and thus did not expect to see this effect. We did, however, observe a negative correlation between recombination rate and introgression/loss of RI under the climate change scenario (Figure 3, Figure S2). This effect is a direct consequence of lower recombination rates leading to increased linkage between RI alleles and globally-adaptive climate alleles. This increased linkage leads in turn to larger numbers of RI alleles being dragged along with globally-adaptive alleles and homogenized between populations. While mutations were not particularly limiting in our simulations, adaptive introgression in regions of low recombination should generally require larger effect alleles than introgression in regions of high recombination, particularly at the onset of climate change when selection is weaker overall.

The strength of climate-mediated selection

A strong shared selection pressure is the key mediator of the collapse of RI we observed. Was the magnitude of simulated selection necessary to cause this collapse realistic? One way to assess this is to measure the magnitude of the phenotypic response to selection in our simulations and compare it to estimates from natural

systems. In our case, the phenotypic response to selection ranged from 0.01-0.06 Haldanes (standard deviations per generation). This is in line with the magnitude of phenotypic response observed in both natural and anthropogenically-induced selection (e.g. Hendry et al. 2008). Further, this is below the theoretical threshold of 0.1 Haldanes thought to result in an unsustainable long-term response to selection (for N_e = 500; Lynch & Lande, 1993; Bürger & Lynch, 1995).

Thus, the strength of selection we modelled was not particularly extreme nor would it necessarily lead to the extinction of the modelled populations. It is also worth noting that the estimated rate of phenotypic change in wild populations due to future GCC is thought to be at least as large as the rates we described here, and are projected to likely exceed 0.1 Haldanes in many cases (Gienapp, Leimu, & Merilä, 2007; Merilä & Hoffman 2016). In sum, the global strength of phenotypic selection simulated here was not unrealistically high, and if anything represents a conservative adaptive scenario.

Conclusion

Hybridization is a double-edged sword under rapid environmental change. It can allow species access to a larger pool of adaptive alleles but linkage with RI alleles will weaken overall RI and may lead to speciation reversal. Importantly, our work highlights the dangers of hybridization for a much wider pool of species, not just those on range margins or with existing porous species boundaries. Our simulations include scenarios where reproductive isolation is initially nearly perfect, and yet is highly degraded through adaptive introgression. Critically, we find a lag between the onset of environmental change and introgression suggesting that present introgression rates

may increase in the future even if the rate of climate change is constant. The end result of climate change may be a world of hybrids as species swap the adaptive alleles they need to survive extinction.

Acknowledgments

This work was supported by an NSERC Banting Postdoctoral Fellowship to GLO and an NSERC Postdoctoral Fellowship to KS. GLO and KS were further supported by postdoctoral funding from Rasmus Nielsen at University of California, Berkeley and Mohamed Noor at Duke University respectively. Matthew Osmund, Kate Ostevik, Rasmus Nielsen and Loren Rieseberg provided helpful feedback and discussions on earlier versions of the manuscript. We thank Philip Messer and Ben Haller for assistance with the SLiM 3.X software.

References

Barton N. H., 1979. The dynamics of hybrid zones. Heredity. 43(3):341–359.

Barton N. H., 2013. Does hybridization influence speciation? Journal of Evolutionary Biology. 26(2):267–269.

Beatty, G.E., Barker L., Chen P.P., Kelleher C.T. & Provan J. 2014. Cryptic introgression into the kidney saxifrage (*Saxifraga hirsuta*) from its more abundant sympatric congener *Saxifraga spathularis*, and the potential risk of genetic assimilation. Annals of Botany. 115(2):179-186.

Boyle, E. A., Li, Y. I., & Pritchard, J. K. 2017. An expanded view of complex traits: from polygenic to omnigenic. Cell. 169(7):1177-1186.

Bürger R. & Lynch M. 1995. Evolution and extinction in a changing environment: a quantitative-genetic analysis. Evolution. 49(1):151-163.

Buerkle, C.A., Morris, R.J., Asmussen, M.A. & Rieseberg, L.H. 2000. The likelihood of homoploid hybrid speciation. Heredity 84: 441–451.

Chunco AJ. 2014 Hybridization in a warmer world. Ecology and Evolution. 4(10):2019-2031.

Clarkson C.S, Weetman D., Essandoh J., Yawson A.E., Maslen G., Manske M., Field S.G., Webster M., Antão T., MacInnis B. & Kwiatkowski D. 2014. Adaptive introgression between Anopheles sibling species eliminates a major genomic island but not reproductive isolation. Nature Communications. 5:4248.

Garroway C.J., Bowman J., Cascaden T.J., Holloway G.L., Mahan C.G., Malcolm J.R., Steele M.A., Turner G. & Wilson P.J. 2010. Climate change induced hybridization in flying squirrels. Global Change Biology. 16(1):113-121.

Gerard P.R., Fernandez-Manjarres J.F., & Frascaria-Lacoste N.A. 2006. Temporal cline in a hybrid zone population between *Fraxinus excelsior* L. and *Fraxinus angustifolia* Vahl. Molecular Ecology. 15(12):3655-3667.

Gienapp P., Leimu R. & Merilä J. 2007. Responses to climate change in avian migration time—microevolution versus phenotypic plasticity. Climate Research. 35(1-2):25-35.

Gómez J.M., González-Megías A., Lorite J., Abdelaziz M. & Perfectti F. 2015. The silent extinction: climate change and the potential hybridization-mediated extinction of endemic high-mountain plants. Biodiversity and Conservation. 24(8):1843-1857.

Gompert, Z., Parchman, T. L., & Buerkle, C. A. 2012. Genomics of isolation in hybrids. Philosophical Transactions of the Royal Society of London B: Biological Sciences. 367(1587):439-450.

Haller B.C. & Messer P.W. 2018. SLiM 3: Forward genetic simulations beyond the Wright–Fisher model, Molecular Biology and Evolution. msy228

Hendry A.P., Farrugia T.J. & Kinnison M.T. 2008. Human influences on rates of phenotypic change in wild animal populations. Molecular Ecology. 17(1):20-29.

Hoffmann A.A. & Sgrò C.M. 2011 Climate change and evolutionary adaptation. Nature. 470(7335):479.

Jump A.S. & Penuelas J. 2005. Running to stand still: adaptation and the response of plants to rapid climate change. Ecology Letters. 8(9):1010-1020.

Lynch, M., & R. Lande. 1993. Evolution and extinction in re-sponse to environmental change. Pp. 234-250 in P. M. Kareiva, J. G. Kingsolver, and R. B. Huey, eds. Biotic interactions and global change. Sinauer, Sunderland, Mass.

Mallet J. 2005. Hybridization as an invasion of the genome. Trends in Ecology & Evolution. 20(5):229-237.

Merilä, J., & Hoffmann, A.A. 2016. Evolutionary Impacts of Climate Change. In *Oxford Research Encyclopedia of Environmental Science*. Oxford University Press.

Oliveira R., Godinho R., Randi E. & Alves P.C. 2008. Hybridization versus conservation: are domestic cats threatening the genetic integrity of wildcats (*Felis silvestris silvestris*) in Iberian Peninsula?. Philosophical Transactions of the Royal Society of London B: Biological Sciences. 363(1505):2953-2961.

Pespeni M.H., Sanford E., Gaylord B., Hill T.M., Hosfelt J.D., Jaris H.K., LaVigne M., Lenz E.A., Russell A.D., Young M.K. & Palumbi S.R. 2013. Evolutionary change during experimental ocean acidification. Proceedings of the National Academy of Sciences. 110(17):6937-6942.

Pfennig KS. 2007. Facultative mate choice drives adaptive hybridization. Science. 318(5852):965-967.

Ravinet M., Faria R., Butlin R.K., Galindo J., Bierne N., Rafajlović M., Noor M.A.F., Mehlig B & Westram, A. M. 2017. Interpreting the genomic landscape of

speciation: a road map for finding barriers to gene flow. Journal of Evolutionary Biology. 30(8):1450-1477.

Rhymer J.M. & Simberloff D. 1996. Extinction by hybridization and introgression. Annual Review of Ecology and Systematics. 27(1):83-109.

Samuk K., Owens G.L., Delmore K.E., Miller S.E., Rennison D.J. & Schluter D. 2017. Gene flow and selection interact to promote adaptive divergence in regions of low recombination. Molecular Ecology. 26(17):4378-4390.

Savolainen O., Lascoux M., & Merilä J. 2013. Ecological genomics of local adaptation. Nature Reviews Genetics. 14(11):807.

Schumer M., Xu C., Powell D.L., Durvasula A., Skov L., Holland C., Blazier J.C., Sankararaman S., Andolfatto P., Rosenthal G.G. & Przeworski, M. 2018. Natural selection interacts with recombination to shape the evolution of hybrid genomes. Science. 360(6389):656-660.

Taylor E.B., Boughman J.W., Groenenboom M., Sniatynski M., Schluter D. & Gow J.L. 2006. Speciation in reverse: morphological and genetic evidence of the collapse of a three-spined stickleback (*Gasterosteus aculeatus*) species pair. Molecular Ecology.15(2):343-355.

Thomas C.D., Cameron A., Green R.E., Bakkenes M., Beaumont L.J., Collingham Y.C., Erasmus B.F., De Siqueira M.F., Grainger A., Hannah L. & Hughes L. 2004. Extinction risk from climate change. Nature. 427(6970):145.

Todesco M., Pascual M.A., Owens G.L., Ostevik K.L., Moyers B.T., Hübner S., Heredia S.M., Hahn M.A., Caseys C., Bock D.G., Rieseberg L.H. 2016. Hybridization and extinction. Evolutionary Applications. 9(7):892-908.

Vallender R., Robertson R.J., Friesen V.L. & Lovette I.J. 2007. Complex hybridization dynamics between golden-winged and blue-winged warblers (*Vermivora chrysoptera* and *Vermivora pinus*) revealed by AFLP, microsatellite, intron and mtDNA markers. Molecular Ecology. 16(10):2017-2029.

Vonlanthen P., Bittner D., Hudson A.G., Young K.A., Müller R., Lundsgaard-Hansen B., Roy D., Di Piazza S., Largiadèr C.R. & Seehausen O. 2012. Eutrophication causes speciation reversal in whitefish adaptive radiations. Nature. 482(7385):357.

Walther G.R., Post E., Convey P., Menzel A., Parmesan C., Beebee T.J., Fromentin J.M., Hoegh-Guldberg O. & Bairlein F. 2002 Ecological responses to recent climate change. Nature. 416(6879):389.

Wickham H. 2016. ggplot2: elegant graphics for data analysis. Springer.

Yeaman S., Hodgins K.A., Lotterhos K.E., Suren H., Nadeau S., Degner J.C., Nurkowski K.A., Smets P., Wang T., Gray L.K., Liepe K.J., Hamann A., Holliday J.A., Whitlock M.C., Rieseberg L.H. & Liepe K.J. 2016. Convergent local adaptation to climate in distantly related conifers. Science. 353(6306):1431-1433.

Zimova M., Mills L.S. & Nowak J.J. 2016. High fitness costs of climate change-induced camouflage mismatch. Ecology Letters. 19(3):299-307.

Supplemental Figures

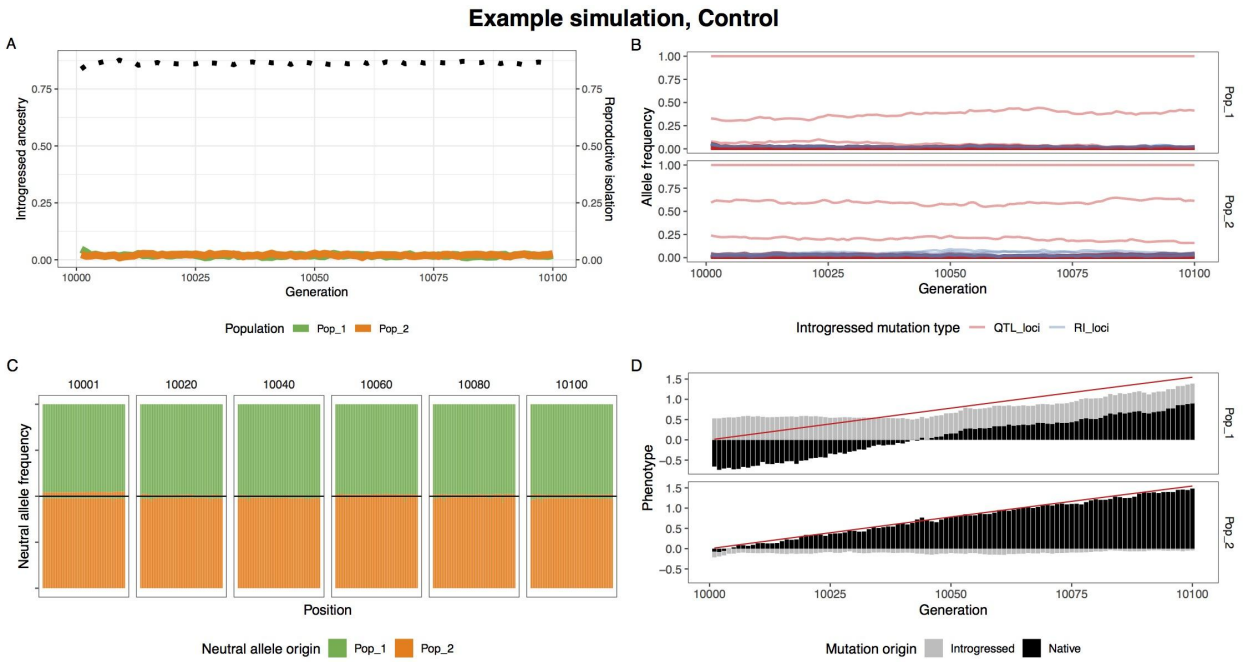

Figure S1 | A single example simulation without climate change, illustrating the lack of introgression. (A) The average introgressed ancestry for each population (orange and green) and the average reproductive isolation between populations (black dotted). (B) The allele frequency trajectory for introgressed climate QTL (red) and RI (blue) alleles. (C) Ancestry for neutral loci during the post-burn in period. The top and bottom halves of the figure represent population 1 and 2 respectively. (D) The optimum phenotype (red line) and the summed phenotypic effect for introgressed and native loci.

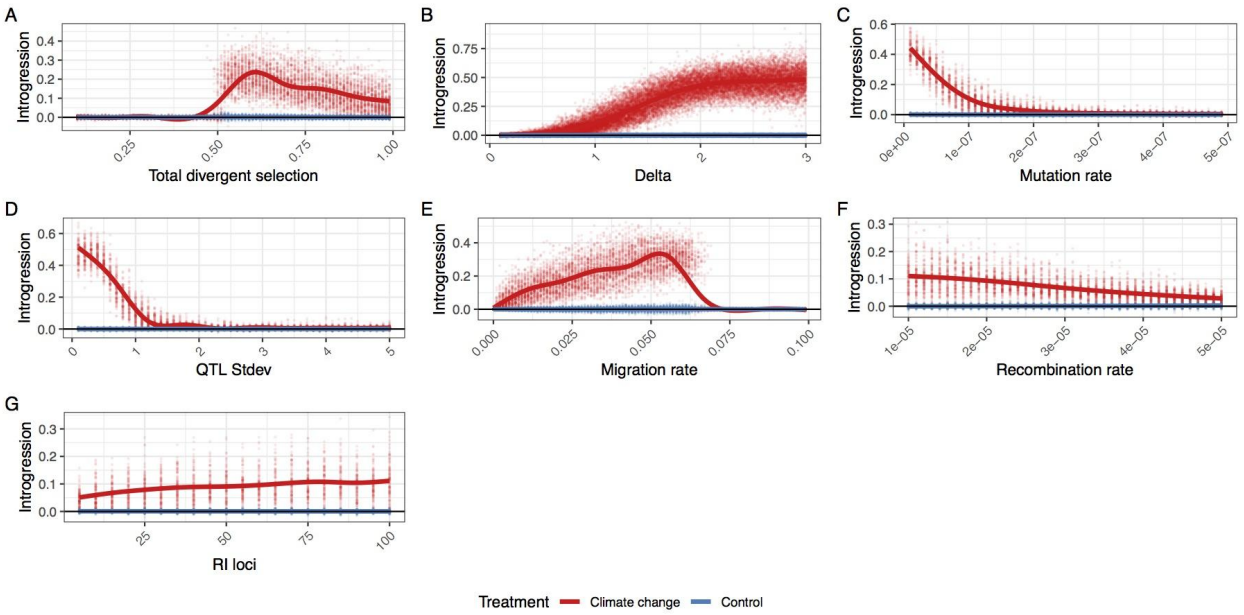

Figure S2 | The average amount of additional introgression at the end of the post-burn in period. Each replicate simulation is represented by two points, one with simulate climate change (red) and one with an extension of the burn in oscillation (blue). Individual parameters were varied to show the effect of (A) total divergent selection, (B) optimum shift per generation (delta), (C) climate QTL mutation rate, (D) climate QTL effect size standard deviation, (E) migration rate, (F) recombination rate and (G) the number of reproductive isolation loci.

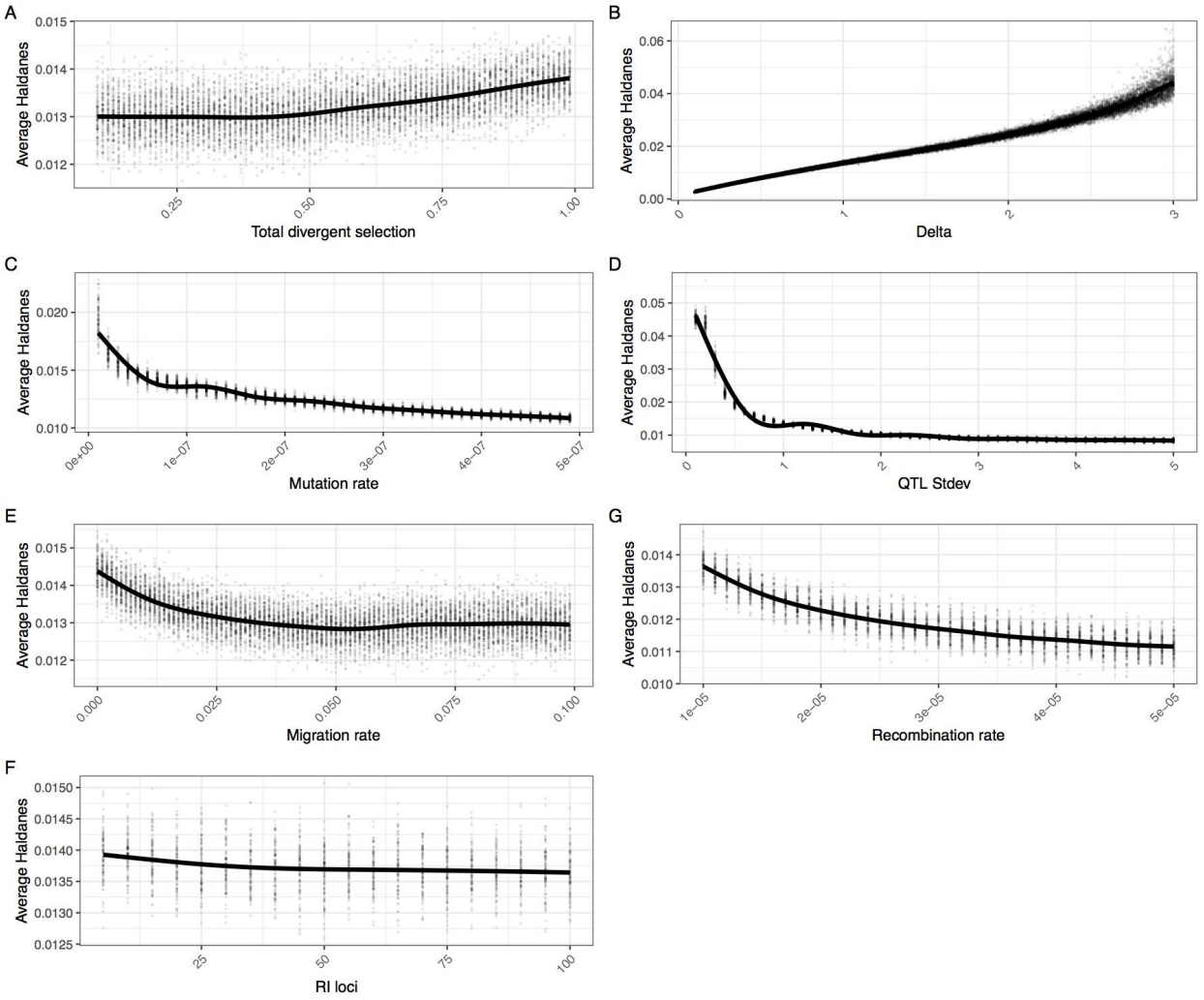

Figure S3 | The average Haldanes for the post-burn in period with climate change. Individual parameters were varied to show the effect of (A) total divergent selection, (B) optimum shift per generation (delta), (C) climate QTL mutation rate, (D) climate QTL effect size standard deviation, (E) migration rate, (F) recombination rate and (G) the number of reproductive isolation loci. Note that Haldanes are scaled by trait variation, so the same rate of absolute phenotypic change (i.e. Darwins) can have multiple different Haldanes if the phenotypic variability changes. This explains why the average Haldanes s decreases with increased mutation rate.

Figure & Table Captions

Figure 1

(A) The genetic architecture of adaptation and speciation in the model. From left to right: Each individual has a single 100-1000 cM chromosome, over which reproductive isolation (RI) loci occur at regularly-spaced intervals. These loci are initialized with RI alleles (at 100% frequency) that confer local adaptation to one of two initial demes (depicted as green or orange alleles, corresponding to deme 1 or deme 2 environments). Both demes are of equal size (Ne = 1000). All non-RI loci (depicted as white/transparent loci, initially) have the potential to give rise to climate-adaptation alleles. The phenotypic effects of each these alleles are drawn from a normal distribution (shown as a gradient from blue to white to red). An individual's climate phenotype is the sum of the phenotypic effects of its climate QTLs (pure additivity). The fitness of each individual is a function of the number of foreign RI alleles and the phenotypic distance of that individual from the environmental optimum, with the climate fitness landscape modelled as a gaussian distribution (shown as a gradient from blue to red). (B) The course of the simulation. Migration rate and population size of the two demes is held constant. In each replicate simulation, the fitness optimum fluctuates regularly a 10 000-generation burn-in period. The state of the initial populations is then duplicated and subjected to 100 additional generations of (1) a climate change scenario in which the climatic optimum rapidly shifts in a single direction and (2) a control scenario in which the optimum continues its fluctuation course. (C) The conditions under which adaptive introgression overwhelms RI. On the left, if the two populations are able to individually track the climatic optimum, newly-arising climate alleles are only able to exert either weakly positive or (more commonly) negative effects on fitness due to overshooting the optimum. In contrast, on the right, if the populations cannot effectively track the optimum (e.g. due to mutational limitations and/or a rapidly shifting optimum), there is scope for climatic alleles to have large positive fitness effects. If these fitness effects are sufficient large, these alleles can overwhelm the negative fitness effects of linked RI alleles and introgress between demes, degrading overall reproductive isolation.

Figure 2

A single example simulation with Δ = 1.5, illustrating the climate driven adaptive introgression. (A) The average introgressed ancestry for each population (orange and green) and the average reproductive isolation between populations (black dotted). (B) The allele frequency trajectory for introgressed climate QTL (red) and RI (blue) alleles. It highlights how RI alleles rise to high frequency in conjunction with climate QTL alleles. (C) Ancestry for neutral loci during the post-burn in period at 20 generation intervals. The top and bottom halves of the figure represent population 1 and 2 respectively. (D) The optimum phenotype (red line) and the summed phenotypic effect for introgressed and native loci.

Figure 3

The average loss of reproductive isolation at the end of the post-burn in period. Each replicate simulation is represented by two points, one with simulating climate change (red) and one with an extension of the burn in oscillation (blue). Individual parameters were varied to show the effect of (A) total divergent selection, (B) optimum shift per generation (delta), (C) climate QTL mutation rate, (D) climate QTL effect size standard deviation, (E) migration rate, (F) the recombination rate and (G)) the number of reproductive isolation loci. The maximum loss of reproductive isolation is 0.9 ($1-s_{Total}$) for most simulations, except when total divergent selection is varied.

Figure S1

A single example simulation without climate change, illustrating the lack of introgression. (A) The average introgressed ancestry for each population (orange and green) and the average reproductive isolation between populations (black dotted). (B) The allele frequency trajectory for introgressed climate QTL (red) and RI (blue) alleles. (C) Ancestry for neutral loci during the post-burn in period. The top and bottom halves of the figure represent population 1 and 2 respectively. (D) The optimum phenotype (red line) and the summed phenotypic effect for introgressed and native loci.

Figure S2

The average amount of additional introgression at the end of the post-burn in period. Each replicate simulation is represented by two points, one with simulate climate change (red) and one with an extension of the burn in oscillation (blue). Individual parameters were varied to show the effect of (A) total divergent selection, (B) optimum shift per generation (delta), (C) climate QTL mutation rate, (D) climate QTL effect size standard deviation, (E) migration rate, (F) recombination rate and (G) the number of reproductive isolation loci.

Figure S3

The average Haldanes for the post-burn in period with climate change. Individual parameters were varied to show the effect of (A) total divergent selection, (B) optimum shift per generation (delta), (C) climate QTL mutation rate, (D) climate QTL effect size standard deviation, (E) migration rate, (F) recombination rate and (G) the number of reproductive isolation loci. Note that Haldanes are scaled by trait variation, so the same rate of absolute phenotypic change (i.e. Darwins) can have multiple different Haldanes if the phenotypic variability changes. This explains why the average Haldanes s decreases with increased mutation rate.

Table 1

Parameters of the adaptive introgression simulations. For each set of simulations, each parameter was set to the starting value which was varied from the minimum to maximum value by the specified increment.

Appendix 1 | Formulas used in adaptive introgression simulations

Optimum during burn in:

$$(1)\ O_{g_{burn}} = sin(\pi g/f)a$$

Optimum during climate shift:

$$(2)\ O_{g_{shift}} = \Delta(g - b)$$

Selection from climate:

$$(3)\ s_{climate\ sample} = 1 - f((\sum_{i=1}^{n} Q_i) - O_g \mid 0, sd_{climate})$$

Selection at RI loci:

$$(4)\ s_{RI} = s_{Total}/l_{RI}$$

Selection from RI:

$$(5)\ s_{RI\ sample} = 1 - \prod_{1}^{n_{RI\ foreign}}(1 - s_{RI})$$

Fitness:

$$(6)\ \omega = s_{RI\ sample} * s_{climate\ sample}$$

Average RI:

$$(7)\ \underline{RI} = ((n_{RI\ p2_{p1}}/n_{RI_{p1}})s_{RI} * 2l_{RI}) - ((n_{RI\ p1_{p2}}/n_{RI_{p2}})s_{RI} * 2l_{RI})$$

Table S1 | List of parameters used in formulas.

Symbol	Parameter
g	Generation number
b	Burn in generations
f	Burn in oscillation wavelength
a	Burn in oscillation amplitude
Q	QTL loci strength
O	Climate optimum
$sd_{climate}$	Standard deviation of gaussian climate fitness function
s_{RI}	Selection at individual RI loci
s_{Total}	Summed strength of selection at all RI loci
l_{RI}	Number of RI loci